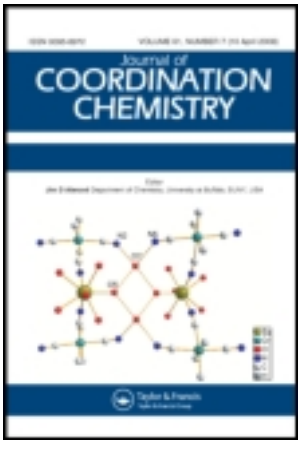

Journal of Coordination Chemistry
Publication details, including instructions for authors and subscription information:
http://www.tandfonline.com/loi/gcoo20

Metal-containing polyurethanes from tetradentate Schiff bases: synthesis, characterization, and biocidal activities

Sumaiya Hasnain [a], M. Zulfequar [b] & Nahid Nishat [a]

[a] Materials Research Lab, Department of Chemistry, Jamia Millia Islamia, New Delhi 110025, India

[b] Materials Research Lab, Department of Physics, Jamia Millia Islamia, New Delhi 110025, India

Published online: 26 Feb 2011.

To cite this article: Sumaiya Hasnain, M. Zulfequar & Nahid Nishat (2011) Metal-containing polyurethanes from tetradentate Schiff bases: synthesis, characterization, and biocidal activities, Journal of Coordination Chemistry, 64:6, 952-964, DOI: 10.1080/00958972.2011.559230

To link to this article: http://dx.doi.org/10.1080/00958972.2011.559230

Journal of Coordination Chemistry
Vol. 64, No. 6, 20 March 2011, 952–964

Taylor & Francis
Taylor & Francis Group

Metal-containing polyurethanes from tetradentate Schiff bases: synthesis, characterization, and biocidal activities

SUMAIYA HASNAIN†, M. ZULFEQUAR‡ and NAHID NISHAT*†

†Materials Research Lab, Department of Chemistry, Jamia Millia Islamia, New Delhi 110025, India
‡Materials Research Lab, Department of Physics, Jamia Millia Islamia, New Delhi 110025, India

(*Received 13 June 2010; in final form 10 January 2011*)

N,*N*′-bis(salicylidene)thiosemicarbazide Schiff base has been synthesized by the reaction of thiosemicarbazide with salicylaldehyde and then reacted with formaldehyde to generate phenolic groups, resulting in the formation of Schiff-base monomeric ligand. It was further incorporated with transition metals, Mn^{+2}, Co^{+2}, Ni^{+2}, Cu^{+2}, and Zn^{+2}, to form Schiff-base metal complex, which was then polymerized with toluene 2,4-diisocyanate to form metal-chelated polyurethanes. Monomeric ligand, its metal complexes, and its metal polychelates were characterized and compared by elemental analysis, FT-IR, ^{1}H NMR, thermal, and biocidal activities to evaluate the enhancement in physical and chemical properties on coordination with metal and on polymerization. SEM images of ligand and polymer metal complexes showed changes in surface morphology, while electronic spectra of polymer metal complexes were used to predict the geometry. Antimicrobial activities were determined by using agar-diffusion method with *Staphylococcus aureus*, *Escherichia coli*, *Bacillus subtilis* (bacteria), *Aspergillus niger*, *Candida albicans*, and *Aspergillus flavus* (yeast). The polymeric ligand had varied antibacterial and antifungal activities, enhanced after chelation and polymerization. Comparative results show that coordination of metal to the ligand enhances its physical and chemical properties which were meliorated on polymerization.

Keywords: Polyurethane; Toluene 2,4-diisocyanate; Schiff base; Biocidal studies

1. Introduction

Coordination polymeric systems to prevent microbial infections, which have become a serious problem in medical devices, drugs, health care, water purifications system, dental surgery equipments, textiles, food packaging, and food storage, have been an active area of research [1–3]. Coordination of these polymers to metal ions increases their biological and pharmaceutical importance. Antimicrobial activity of coordination polymers depends on the central metal ion and the nature of the ligand. Modification of polyurethanes by the incorporation of metal and functional groups can improve various desired properties of materials such as enhanced thermal stability, flexibility, and stability. The properties lead to a variety of applications, for example Nanjundan *et al.* [4, 5]

*Corresponding author. Email: nishat_nchem08@yahoo.com

ISSN 0095-8972 print/ISSN 1029-0389 online © 2011 Taylor & Francis
DOI: 10.1080/00958972.2011.559230

prepared metal-containing polyurethane-urea possessing good flame-retardant property by the reaction of hexamethylene diisocyanate (HMDI) or toluene 2,4-diisocyanate (TDI) with salts of mono(hydroxyl butyl) hexolic acid with divalent metals. Schiff-base polyurethanes have also been established [6, 7] and thiosemicarbazide and thiosemicarbazone Schiff bases have gained special attention due to their activity against protozoa, influenza, small pox, malaria, cancer, and tuberculosis [8]. Recently, we synthesized a series of antimicrobial coordination polymers which possess promising antimicrobial properties [9–12]. Owing to the wide range of microbial properties of thiosemicarbazides and their ability to form chelates with metal ions, in this study we report the syntheses and characterizations of metal-containing polyurethanes.

2. Experimental

Thiosemicarbazide and TDI were purchased from S.D. fine chemical Ltd., salicyaldehyde, formaldehyde (37–41%) and dimethyl sulfoxide (DMSO) from Merck, India, manganese(II)acetate tetrahydrate [$Mn(CH_3COO)_2 \cdot 4H_2O$], cobalt(II)acetate tetrahydrate [$Co(CH_3COO)_2 \cdot 4H_2O$], nickel(II)acetate tetrahydrate [$Ni(CH_3COO)_2 \cdot 4H_2O$], copper(II)acetate monohydrate [$Cu(CH_3COO)_2 \cdot H_2O$], and zinc(II)acetate dihydrate [$Zn(CH_3COO)_2 \cdot 2H_2O$] from Qualigens fine chemicals, India.

2.1. *Measurements*

Elemental analyses of C, H, N, and S were carried out on an elemental analyzer system GmbH Vario ELIII, while the percentage of metal was obtained by complexometric titration with EDTA after decomposing with concentrated nitric acid (HNO_3) at room temperature. Magnetic susceptibility measurements were recorded on a vibrating sample magnetometer model 155 at room temperature. Fourier transform-infrared (FT-IR) spectra were obtained on a Perkin-Elmer IR spectrophotometer model 621 using KBr pellets. Nuclear magnetic resonance spectra (^{1}H NMR) were recorded on a JEOL-GSX 300 MHz FX 1000 FT NMR spectrometer using DMSO as a solvent and tetramethylsilane (TMS) as an internal standard. UV-Vis spectra were obtained on a Perkin-Elmer Lambda EZ-201 spectrophotometer using DMSO. Thermal behavior was demonstrated by using Perkin-Elmer (Pyris Diamond) thermal analyzer in nitrogen at heating rate of $20^\circ C\,min^{-1}$. Solubility of the polymers and polymer metal complexes was determined in both polar and non-polar solvents, while antimicrobial activity tests were performed using agar well diffusion and the number of viable cells was counted by utilizing the spread plate method [13]. Test samples were prepared using DMSO as solvent at 50 and $100\,\mu g\,mL^{-1}$ for bacteria and fungi, respectively.

2.2. *Synthesis*

2.2.1. Synthesis of monomeric ligand (STF). Thiosemicarbazide (0.01 mol, 0.91 g) was dissolved in a minimum of distilled water in a 250 mL three-necked round bottom flask and was attached to an ice-cooled reflux condenser with a magnetic stirrer and

maintained at 70°C. Salicylaldehyde (0.02 mol, 2.44 g) was dissolved in 20 mL ethanol and added drop wise using a burette to the thiosemicarbazide solution and stirred continuously for 1.5 h. This is a very fast reaction and as soon as salicylaldehyde was added, a light yellow precipitate appears. It was then filtered, washed with distilled H_2O and diethyl ether, and dried at 30–40°C for 8 h to give *N*,*N*′-bis(salicylidene)thiosemicarbazide Schiff base.

The dried Schiff base was dissolved in DMSO, formaldehyde (37–40%) (0.2 mol, 0.15 mL) was added to this hot solution and the reaction mixture was heated at 70°C for 2 h. Monomeric light yellow STF was obtained after washing with diethyl ether and drying at 40°C. Melting point is 86°C.

2.2.2. Synthesis of chelated monomers [STF–M(II)]. A series of transition metal complexes [Mn(II), Co(II), Ni(II), Cu(II), and Zn(II)] were prepared from STF. Procedure for the preparation of [STF–Zn(II)] complex are as follows.

STF (0.01 mol, 3.13 g) was dissolved in 20 mL DMSO and heated at 60°C in a round bottom flask fitted to an ice-cooled condenser. Zinc(II) salt (0.01 mol, 2.19 g) dissolved in DMSO was added to this hot solution and heated for 8 h at the same temperature giving a light orange, viscous solution which was precipitated in distilled water, filtered, and washed several times with distilled H_2O and diethyl ether to remove uncomplexed metal ions. It was then oven dried at 45°C for 24 h to obtain light orange [STF–Zn(II)]. Similar procedure was adopted for the preparation of complexes of Mn(II), Co(II), Ni(II), and Cu(II). Synthetic route to metal complexes is represented in scheme 1.

Elemental analysis data and FT-IR spectral bands are tabulated in tables 1 and 2, respectively, while thermal and antimicrobial activities have been represented in figure 1(a) and (b) and "Supplementary material" and described in respective sections.

2.2.3. Synthesis of metal-chelated polyurethane [PUT–M(II)]. Metal-containing bifunctional monomer [STF–M(II), where M = Mn(II), Co(II), Ni(II), Cu(II), and Zn(II), 0.01 mol] was dissolved in 30 mL DMSO in a 250 mL three-necked round bottom flask. Temperature of the flask was increased to 80°C and stirred magnetically. Then 1.74 mL (0.01 mol) of TDI was added to this solution in the presence of 2–3 drops of di-*n*-butyltindilaurate (DBTDL) as catalyst. The reaction mixture was stirred at this temperature for 6 h, then precipitated and washed with distilled water, diethyl ether, and dried at room temperature for 24 h to give metal-chelated polyurethane [PUT–M(II)]. Color and % yield of the metal-containing polyurethanes are listed in table 1. Synthetic route to metal-containing polyurethane is represented in scheme 2.

2.3. *Antimicrobial assessment*

Antimicrobial activities of the synthesized compounds were tested against various microorganisms in DMSO. Sample concentrations of 50 and 100 $\mu g\,mL^{-1}$ were taken for antibacterial and antifungal studies, respectively. Antibacterial activity was screened against *Staphylococcus aureus*, *Bacillus subtilis* (Gram positive), and *Escherichia coli* (Gram negative), while antifungal screening was done against *Aspergillus niger*, *Candida albicans*, and *Aspergillus flavus*.

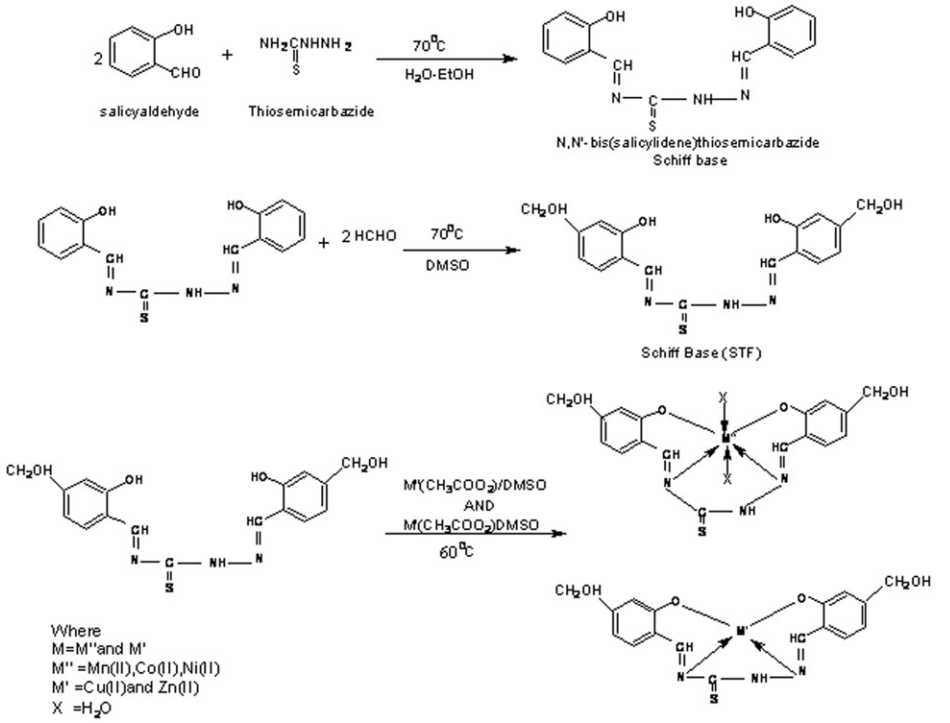

Scheme 1. Synthesis of moneric ligand [STF–M(II)].

Bacterial strains were nourished in a nutrient broth (Difco) and yeasts in malt extract broth (Difco), and incubated for 24 and 48 h, respectively. According to the agar-diffusion method, bacteria were incubated on Mueller–Hinton agar and yeast on Sabouraud dextrose agar. Wells were dug in the media with the help of a sterile steel borer and 0.1 mL of each sample was introduced in the corresponding well. Standard drugs, kanamycin and miconazole, were taken as control for bacteria and fungi, respectively. Zones of inhibition on the plates were measured in millimeters. Depending on the diameters and clarity of the zones of inhibition they are regarded as inactive, moderately active, and highly active, as represented in table 3 and figure 1(a) and (b).

3. Results and discussion

Monomeric ligand and its metal polychelates were synthesized by the reaction of thiosemicarbazide with salicylaldehyde, then formaldehyde was reacted to generate phenolic groups in the formed Schiff base. The ratio of formaldehyde to Schiff base must be 1 : 1 in order to avoid polymerization [14]. Thereafter, Mn(II), Co(II), Ni(II), Cu(II), and Zn(II) complexes were prepared. Elemental analyses revealed that metal : ligand molar ratio is 1 : 1 and the ligand is tetradentate. Oxygen of salicylaldehyde and nitrogen of thiosemicarbazide are involved in coordination with Cu(II), and Zn(II) with H_2O also involved in coordination with Mn(II), Co(II), and

Table 1. Elemental and physical analysis data.

Compound abbreviation	Empirical formula	Elemental analysis[a] (%)					Color	% Yield (approx.)
		Carbon	Hydrogen	Nitrogen	Sulfur	Metal		
STF	($C_{17}H_{17}N_3O_4S$)	56.81 (55.91)	4.76 (4.34)	11.69 (11.47)	8.92 (8.62)	–	Light yellow	79.4
STF–Mn(II)	($C_{17}H_{19}N_3O_6S$–Mn)–(H_2O)$_2$	45.54 (44.70)	4.27 (4.12)	9.37 (8.88)	7.15 (6.50)	12.25 (11.69)	Mustard	78
PUT–Mn(II)	($C_{26}H_{25}N_5O_8S$–Mn)–(H_2O)$_2$	50.16 (50.09)	4.04 (4.05)	11.25 (11.21)	5.15 (5.11)	8.82 (8.73)	Dark yellow	76
STF–Co(II)	($C_{17}H_{19}N_3O_6S$–Co)–(H_2O)$_2$	45.13 (44.39)	4.23 (3.92)	9.28 (9.11)	7.08 (7.00)	13.02 (12.77)	Blackish brown	77
PUT–Co(II)	($C_{26}H_{25}N_5O_8S$–Co)–(H_2O)$_2$	49.84 (50.06)	4.02 (4.12)	11.17 (11.14)	5.11 (5.16)	9.40 (9.31)	Brown	72
STF–Ni(II)	($C_{17}H_{19}N_3O_6S$–Co)–(H_2O)$_2$	45.16 (44.41)	4.26 (4.01)	9.29 (8.64)	7.09 (6.80)	12.98 (11.21)	Brown	79
PUT–Ni(II)	($C_{26}H_{25}N_5O_8S$–Ni)–(H_2O)$_2$	49.79 (50.08)	4.01 (4.04)	11.16 (11.11)	5.11 (5.19)	9.35 (9.35)	Dark orange	77
STF–Cu(II)	($C_{17}H_{15}N_3O_4S$–Cu)	48.50 (47.82)	3.59 (3.20)	9.98 (9.01)	7.61 (6.28)	15.09 (14.37)	Grayish green	76
PUT–Cu(II)	($C_{26}H_{21}N_5O_6S$–Cu)	52.47 (52.41)	3.55 (3.52)	11.76 (11.75)	5.38 (5.41)	10.67 (10.63)	Green	72
STF–Zn(II)	($C_{17}H_{15}N_3O_4S$–Zn)	48.29 (47.55)	3.57 (2.98)	9.93 (9.00)	7.58 (6.77)	15.46 (14.21)	Light orange	78
PUT–Zn(II)	($C_{26}H_{21}N_5O_6S$–Zn)	52.31 (53.47)	3.54 (3.54)	11.73 (11.65)	5.37 (5.45)	10.95 (10.86)	Yellow	68

[a]Calculated (observed) value.

Table 2. Important FT–IR spectral bands.

Assignments	STF	STF–Mn(II)	STF–Co(II)	STF–Ni(II)	STF–Cu(II)	STF–Zn(II)	PUT–Mn(II)	PUT–Co(II)	PUT–Ni(II)	PUT–Cu(II)	PUT–Zn(II)
OH	3424(b)	3420(m)	3418(m)	3418(m)	3420(m)	3420(m)	–	–	–	–	–
Phenolic (–CO)	1307	1289(m)	1291(m)	1286(m)	1288(m)	1286(m)	1289(m)	1291(m)	1286(m)	1288(m)	1286(m)
CH_2 (bending)	1402	1401	1400	1402	1402	1400	1398	1395	1397	1397	1396
N–H (stretching)	3350(b)	3350(m)	3350(m)	3350(m)	3350(m)	3350(m)	3350(m)	3350(m)	3350(m)	3350(m)	3350(m)
N–H (bending)	1542(s)	1537(s)	1540(s)	1538(s)	1535(s)	1540(s)	1537(s)	1540(s)	1538(s)	1535(s)	1540(s)
C=S (stretching) + C=C (bending)	715(m)	707(m)	705(m)	711(m)	711(m)	708(m)	707(m)	705(m)	711(m)	711(m)	708(m)
C=C (aromatic stretching)	1536–1539(s)	1536–1539(s)	1536–1539(s)	1536–1539(s)	1536–1539(s)	1536–1539(s)	1536–1539(s)	1536–1539(s)	1536–1539(s)	1536–1539(s)	1536–1539(s)
CH=N + (C=O–O in PUT only)	1620	1602(s)	1600(s)	1600(s)	1606(s)	1604(s)	1600–1636(s)	1600–1636(s)	1600–1636(s)	1600–1636(s)	1600–1636(s)
C–N	1434(s)	1437(s)	1434(s)	1435(s)	1434(s)	1434(s)	1438(b)	1437(b)	1439(b)	1440(b)	1438(b)
M–N	–	449(s)	442(s)	446(s)	458(s)	452(s)	449(s)	442(s)	446(s)	458(s)	452(s)
M–O	–	510(m)	517(m)	511(m)	515(m)	510(m)	510(m)	517(m)	511(m)	515(m)	510(m)
M–H_2O (rocking)	–	992	985	988	–	–	992	985	988	–	–
M–H_2O (wagging)	–	747	740	758	–	–	747	740	758	–	–

(s) Strong, (m) medium, (b) broad, (w) weak.

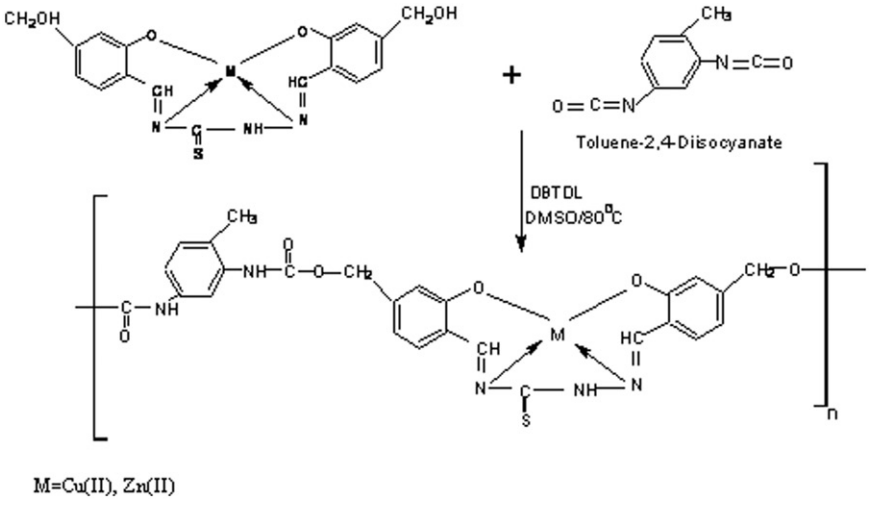

Scheme 2. Synthesis of metal chelated polyurethane [STF–M(II)].

Ni(II) complexes. Polyaddition of TDI with SFT-M(II) was done in the presence of DBTDL to obtain metal-chelated polyurethane [PUT–M(II)]. Reaction between diols and diisocyanates was catalyzed by DBTBL and takes place *via* the formation of a ternary complex between the reagents and the catalyst [15].

3.1. *FT-IR analysis*

Comparison of FT-IR spectra STF–M and PUT–M(II) are illustrated in table 2. Azomethine shows absorptions at 1620 in STF which was lowered by 14–20 cm^{-1} in STF–M; in PUT–M this absorption was somewhat broadened in the range 1600–1636 cm^{-1} due to the overlapping of carbonyl stretching (–C=O) peaks of the urethane group with azomethine. Negative shift in the IR frequency indicates the coordination of metal through the azomethine nitrogen [16]. OH stretch in STF was observed as a very broad peak at 3424 cm^{-1} due to phenol, but in STF–M, a less broad peak was observed at 3313 cm^{-1} due to aliphatic alcohol, while in PUT–M, these peaks were absent, showing that aliphatic OH is involved in polyurethane formation and aromatic OH is involved in metal bond formation. Confirmation of metal bond formation is obtained by the negative shift of phenolic C–O stretch, which appeared at 1307 cm^{-1} in STF and between 1286 and 1291 cm^{-1} in polymeric metal complexes and metal-chelated polyurethanes [17]. Peaks at 1536–1539 cm^{-1} are attributed to aromatic C=C stretch, while C=S is overlapped with C=C bending vibrations at 705–711 cm^{-1}. No peak is observed at 2600–2400 cm^{-1} which shows that thiosemicarbazide remains in its thio-keto form [18]. Characteristic peak at 3350 cm^{-1} is due to –NH stretching and at 1540–1535 cm^{-1} to NH bending of the urethane group. Coordination of metal ion is further supported by the appearance of M–O stretches at 510–517 cm^{-1} [19] and M–N stretches at 442–458 cm^{-1} [20]. Medium to weak intensity bands due to coordinated water (M–H_2O) are at 985–992 cm^{-1} (rocking) and 740–758 cm^{-1} (wagging) in spectra of

Mn(II), Co(II), and Ni(II) polymeric metal complexes, showing coordinated water in these polychelates.

3.2. *NMR analysis*

Comparison of ^{1}H NMR spectra of STF, STF–Zn(II), and PUT–Zn(II) shows the proposed structures. ^{1}H NMR analysis was done in DMSO-d_6, whose signal was observed as a very sharp singlet at 2.48–2.66 ppm. Signals for imine protons (–CH=N–) were observed at 8.31 ppm (2H, 2.44 J, s) for STF, at 7.91 ppm (2H, 2.10 J, s) for STF–Zn(II), and at 7.90 ppm (2H, 2.00 J, s) for PUT–Zn(II). Protons of thiosemicarbazide (–NH–) appeared at 7.14 ppm (1H, 7.22 J, s) for STF and 7.12 ppm (1H, 7.20 J, s) for STF–Zn(II), respectively. In PUT–Zn(II), thiosemicarbazide NH signal was merged with the urethane (–NH–C=O–O–) to give a signal at 7.00 ppm (3H, 7.45 J, m) [21]. Methyl protons appeared at 2.24 ppm (3H, 0.79 J, d) for PUT–Zn(II) while methylene appeared at 3.32 ppm (4H, 1.00 J, d) in STF, at 3.31 ppm (4H, 1.04 J, d) in STF–Zn(II), and at 3.52 ppm (4H, 2.83 J, s) for PUT–Zn(II). Signals for aromatic protons were in the range of 6.80–7.71 ppm (6H, m) in the ligand and zinc metal complex, while 6.68–7.90 ppm (9H, m) in polymer metal complex. Characteristic peak at 10.80 ppm (4H, 3.83 J, very broad signal) was due to phenolic –OH in STF, while in STF–Zn(II) it was observed at 11.6 ppm (2H, 2.91 J, triplet and less broad) and was completely absent in PUT–Zn(II), showing the coordination of zinc to the phenol.

3.3. *UV-Vis analysis*

Electronic spectra of the synthesized polymers were recorded in DMSO. Various crystal field parameters $10D_q$, B, β, and β° have been calculated (table 4). The magnetic moment of PUT–Mn(II) is 5.68 B.M. [22] corresponding to five unpaired electrons. The electronic spectrum exhibits three absorptions at 16,200, 19,400, and 22,980 cm^{-1}, assigned to $^4T_{1g}(G) \leftarrow {}^6A_{1g}(F)$, $^4T_{2g}(G) \leftarrow {}^6A_{1g}(F)$, and $^4E_g(G) \leftarrow {}^6A_{1g}(F)$ transitions, respectively, suggesting high spin octahedral geometry. The polymer metal complex of Co(II) had magnetic moment of 4.52 B.M. [23] due to four unpaired electrons and electronic transitions at 9200, 17,200, and 27,520 cm^{-1} corresponding to $^4T_{2g}(F) \leftarrow {}^4T_{1g}(F)$, $^4A_{2g}(P) \leftarrow {}^4T_{1g}$, and $^4T_{1g}(P) \leftarrow {}^4T_{1g}(F)$, respectively, indicative of octahedral geometry. Magnetic moment of PUT–Ni(II) is 2.94 B.M. [24]. Three bands were observed at 9628, 13,977, and 24,042 cm^{-1} corresponding to $^3T_{2g} \leftarrow {}^3A_{2g}$, $^3T_{1g} \leftarrow {}^3A_{2g}$, and $^3T_{1g}(P) \leftarrow {}^3A_{2g}$ transitions, respectively, suggestive of octahedral complex. PUT–Cu(II) has magnetic moment of 1.71 B.M. with bands at 14,980 and 23,520 cm^{-1} assigned to $^2A_{1g} \leftarrow {}^2B_{1g}(F)$ and charge transfer, respectively, indicative of square-planar geometry [25]. In the polymeric Zn(II) complex the spectrum was ligand related; we suggest tetrahedral geometry.

3.4. *Scanning electron microscopy*

Scanning electron microscope is used to investigate the surface morphology of STF and PUT–Ni as depicted (Supplementary material). SEM of STF reveals a brittle, glassy, and crystalline structure. Layers in the micrograph reveal that the system contains

Table 3. Comparative antimicrobial data.

	E. coli	S. aureus	*B. subtilis*	*C. albicans*	*A. niger*	*A. flavus*
STF	6 ± 1	5 ± 1	3 ± 1	4 ± 1	6 ± 1	2 ± 1
STF–Mn(II)	17 ± 1	5 ± 2	11 ± 1	4 ± 1	3 ± 1	7 ± 1
PUT–Mn(II)	21 ± 0.5	9 ± 1	18 ± 1	9 ±	8 ± 1	11 ± 1
STF–Co(II)	8 ± 1	11 ± 2	7 ± 1	10 ± 1	11 ± 1	11 ± 1
PUT–Co(II)	12 ± 2	15 ± 1	10 ± 1	15 ± 1	18 ± 1	19 ± 0.5
STF–Ni(II)	6 ± 1	12 ± 1	9 ± 1	6 ± 1	9 ± 2	11 ± 1
PUT–Ni(II)	10 ± 0.06	20 ± 1	16 ± 1	11 ± 1	15 ± 0.6	17 ± 1
STF–Cu(II)	17 ± 1	15 ± 1	14 ± 2	16 ± 1	13 ± 1	17 ± 1
PUT–Cu(II)	21 ± 1	18 ± 1	20 ± 1	20 ± 2	18 ± 1	23 ± 1
STF–Zn(II)	6 ± 1	7 ± 0.5	6 ± 1	18 ± 0.6	17 ± 1	16 ± 1
PUT–Zn(II)	11 ± 1	16 ± 1	15 ± 1	24 ± 1	25 ± 1	21 ± 1
Kanamycin	25	25	24	–	–	–
Miconazole	–	–	–	27	27	25

Zone of inhibition (mm) ± standard deviation.

Table 4. Magnetic susceptibility, electronic spectral, and their ligand field parameters.

Abbreviation	Magnetic moment (μ_{eff})	Electronic transitions (cm^{-1})	Assignment	10Dq	*B*	β	β°
PUT–Mn(II)	5.68	22980	$^4E_g(G) \leftarrow {}^6A_{1g}(F)$	4178.6	835.72	0.87	0.13
		19400	$^4T_{2g}(G) \leftarrow {}^6A_{1g}(F)$				
		16200	$^4T_{1g}(G) \leftarrow {}^6A_{1g}(F)$				
PUT–Co(II)	4.52	27520	$^4T_{1g}(P) \leftarrow {}^4T_{1g}$	7284.6	809.41	0.83	0.17
		17200	$^4A_{2g}(P) \leftarrow {}^4T_{1g}$				
		9200	$^4T_{2g} \leftarrow {}^4T_{1g}$				
PUT–Ni(II)	2.94	24042	$^3T_{1g}(P) \leftarrow {}^3A_{2g}$	9278.5	843.57	0.78	0.22
		13977	$^3T_{1g} \leftarrow {}^3A_{2g}$				
		9628	$^3T_{2g} \leftarrow {}^3A_{2g}$				
PUT–Cu(II)	2.21	23520	$^2A_{1g} \leftarrow {}^2B_{1g}$	–	–	–	–
		14980					

μ_{eff} = effective magnetic moment in B.M.

several polymer chains arranged in a well-defined pattern. The fractured surface shows homogeneity in the polymeric system, thus reactants have reacted completely to form a clear homogenous polymer.

The structure of PUT–Ni(II) shows clearly visible fine globular structures. Heterogeneity in the scanning electron micrographs shows incorporation of nickel to the polymeric ligand, which confirms incorporation of the inorganic and organic moieties.

3.5. *Thermal analysis*

Thermal stability of polymer metal complexes is strongly dependent on the structure of the polymeric ligand and on the mode of complexation, being higher or lower [26] than that of the polymer itself, therefore thermal degradation of the ligand, metal complex, and metal-chelated polyurethane were compared; degradation behavior is shown in Supplementary material. The study range was from 0 to 800°C. All polychelates and

metal-chelated polyurethanes show slight differences in their thermal behavior. TGA curve for STF shows continuous degradation with increase in temperature and all sample was decomposed at 500°C, while the TG curves of PUT–Cu(II) indicate two step degradation, which is perhaps because the non-coordinated part of the polymer decomposes first while the coordinated part decomposes later. In STF–Mn(II), STF–Cu(II), PUT–Mn(II), and PUT–Cu(II) decomposition just above 100°C was due to the evolution of adsorbed and coordinated water. Decomposition at 210–280°C is attributed to non-coordinated organic backbone of the polymers. Polyurethane decomposition occurs in one step starting at 220°C, typical of urethane [27] due to the breaking of polymeric linkages. Gradual but continuous decrease in weight is observed above 300°C, due to the loss of coordinated part. At 700°C, 80–90% weight loss is observed. Comparison of the data reveals that PUT–Cu(II) shows greatest stability, due to the higher stability constant of Cu(II).

3.6. *Antibacterial activity of metal-chelated polyurethanes*

Modes of action of metal ions in biological processes are often complex but are believed to involve bonding to heterocyclic residues of biological molecules, i.e., proteins, enzymes, nucleic acids, etc. Ligand, metal complexes, and metal-chelated polyurethanes were screened for antibacterial activity against two Gram-positive bacteria, i.e., *S. aureus*, *B. subtilis*, and one Gram-negative bacteria, i.e., *E. coli*, by zones of inhibition (figure 1a). All metal-chelated polyurethanes are more active than their corresponding metal complexes and PUT–Cu(II) is more active than other metal-chelated polyurethanes.

Antifungal activity of the ligand and metal-containing polyurethanes was studied against *A. niger*, *C. albicans*, and *A. flavus* (figure 1b). PUT–Zn(II) shows the highest zone of inhibition against *C. albicans* and *A. niger*, while PUT–Cu(II) shows highest inhibition against *A. flavus*. PUT–Co(II) and PUT–Ni(II) show moderate activity against all fungi but PUT–Mn(II) is almost inactive for all the yeasts under study. All metal complexes and ligand were less active than their corresponding polyurethanes. Comparative data have been tabulated in table 3.

It has been suggested that compounds with nitrogen and oxygen donor systems inhibit enzyme production, as enzymes which require a free hydroxyl group for their activity are especially susceptible to deactivation by ions of complexes [28]. Coordination reduces the polarity of the central metal ion and increases lipophilic nature, favoring permeation through the lipid layer of the membrane. Lethal action of isocyanate biocides is an outcome of their ability to inhibit microbes. Low concentrations of isocyanate are sporostatic and inhibit germination. It is difficult to pinpoint accurately the mechanism(s) responsible for isocyanate-induced microbial inactivation. Higher activity of Gram-positive bacteria can be explained on the basis that there is a thick outer membrane made up of lipopolysaccharide and protein in the Gram-negative bacteria which inhibit or partially permit penetration of polymer metal complexes into the bacterial cell, but this type of membrane is not present in Gram-positive bacteria, where a wall of peptidoglycan is present which easily permits penetration of polymer metal complexes thus inhibiting its life-sustaining activities. Several other mechanisms for the inhibition of microbes have also been reported [29]. Studies regarding the biocidal activities of polymers containing diisocyanates have been published recently

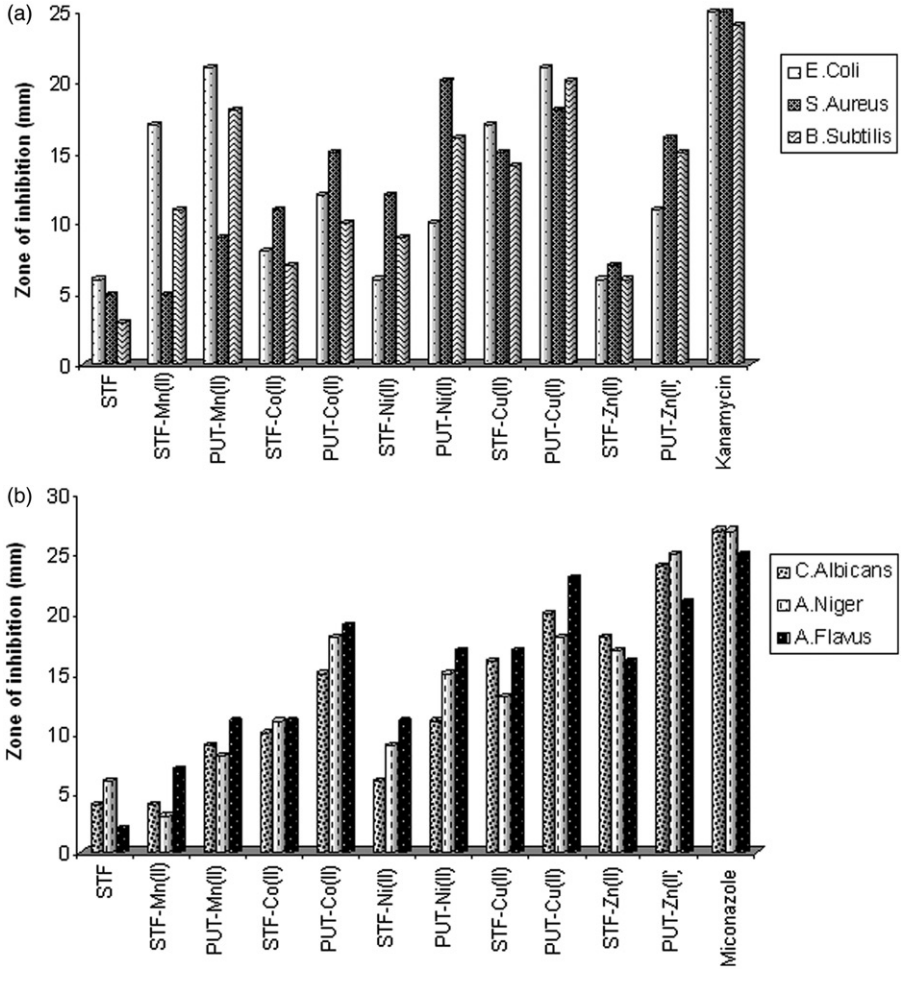

Figure 1. (a) Antibacterial and (b) antifungal assessment.

[30, 31], which show their potential to be used in a variety of biomedical applications. Therefore, the interactive and cross-linking property of diisocyanate must play a considerable role in this biocidal activity.

4. Conclusions

Schiff-base containing metals in the main chain underwent polymerization to give metal-chelated polyurethanes in good yield. Polymeric ligand to metal ion ratio was 1 : 1 in all cases. Spectral data reveal nitrogen of thiosemicarbazide and oxygen of –OH are involved in coordination with Cu(II) and Zn(II) giving them square planar and tetrahedral geometries, respectively, while two waters were also involved in the

coordination of Mn(II), Co(II), and Ni(II) giving them octahedral structure. Surface morphologies of the ligand and its polychelate show the change in surface appearance after incorporation of metal. In comparison to other recently reported Schiff bases of salicylaldehyde and diamines and metal complexes [32], our metal complexes exhibited better biocidal effects. The recent work of Raman *et al*. [33] on intercalative DNA binding with complexes and enhancement in the thermal stability and biocidal activity against pathogenic bacteria and fungi encourage us to further modify these compounds which can be used for medical and biomaterial applications.

Acknowledgments

S. Hasnain wish to thank the Council of Scientific and Industrial Research (CSIR), New Delhi, for financial support in the form of the Senior Research Fellowship, and thanks are also due to Sophisticated Analytical Instrument Facility (SAIF), AIIMS, New Delhi, for providing SEM facility.

References

[1] H.H. Balkhy, G. Cunningham, F.K. Chew, C. Francis, D.J. Al Nakhli, M.A. Almuneef, Z.A. Memish. *Int. J. Infect. Dis.*, **10**, 326 (2006).
[2] E.S. Park, H.J. Lee, H.Y. Park, M.N. Kim, K.H. Chung, J.S. Yoon. *J. Appl. Polym. Sci.*, **80**, 728 (2001).
[3] L. Dussart, J.P. Dupont, I. Zimmerlin, M. Lacroix, J.M. Saiter, G.A. Junter, T. Jouenne. *Water Res.*, **37**, 1593 (2003).
[4] R. Jayakumar, S. Nanjundan, M. Prabaharan. *React. Funct. Polym.*, **66**, 299 (2006).
[5] R. Jakumar, Y.S. Lee, S. Nanjundan. *React. Funct. Polym.*, **55**, 267 (2003).
[6] N. Senthilkumar, A. Raghavan, A.S. Nasa. *Macromol. Chem. Phys.*, **206**, 2490 (2005).
[7] M.J.M. Campbell. *Coord. Chem. Rev.*, **15**, 279 (1975).
[8] D.J. Bauer, L.S. Vincent, C.H. Kempe, A.W. Downe. *Lancet*, **2**, 494 (1963).
[9] S. Parveen, T. Ahamad, A. Malik, N. Nishat. *Polym. Adv. Technol.*, **19**, 1779 (2008).
[10] T. Ahamad, V. Kumar, N. Nishat. *J. Biomed. Mater. Res. Part A*, **88A**, 288 (2008).
[11] N. Nishat, T. Ahamad, M. Zulfequar, S. Hasnain. *J. Appl. Polym. Sci.*, **110**, 3305 (2008).
[12] T. Ahamad, V. Kumar, N. Nishat. *Polym. Int.*, **55**, 1398 (2006).
[13] C.H. Collins, P.M. Lyne. *Microbial Methods*, University Park Press, Baltimore (1970).
[14] C.S. Marvel, N. Tarkoy. *J. Am. Chem. Soc.*, **79**, 6000 (1957).
[15] S.J. Angyal, J. Morris, R. Tetaz, J.G. Wilson. *J. Chem. Soc.*, **3**, 2141 (1950).
[16] M. Joseph, M. Kuriakose, M.R.P. Kurup, E. Suresh, A. Kishore, S.G. Bhat. *Polyhedron*, **25**, 61 (2006).
[17] M. Tunçel, A. Ozbulbul, S. Serın. *React. Funct. Polym.*, **68**, 292 (2008).
[18] A.A. El-asmy, K.M. Ibrahim, M.M. Bekheit, M.M. Mostafa. *Synth. React. Inorg. Met. Org. Chem.*, **15**, 287 (1985).
[19] K.C. Gupta, A.K. Sutar. *J. Appl. Polym. Sci.*, **108**, 3927 (2008).
[20] M.K. Singh, A. Das, B. Paul. *J. Coord. Chem.*, **62**, 2745 (2009).
[21] M. Barikani, M. Mohammadi. *Carbohydr. Polym.*, **68**, 773 (2007).
[22] V.N. Patange, B.R. Arbad. *Transition Met. Chem.*, **32**, 944 (2007).
[23] A.B.P. Lever. *Inorganic Electronic Spectroscopy*, Elsevier Publishing Company, London (1968).
[24] F.A. Cotton, G. Wilkinson, C. Murillo, M. Bochmann. *Advanced Inorganic Chem.*, 6th Edn, Wiley Interscience, New York (1999).
[25] M.P. Sathisha, U.N. Shetti, V.K. Revankar, K.S.R. Pai. *Eur. J. Med. Chem.*, **43**, 2338 (2008).
[26] E.S. Dragan, M.V. Dinu, G. Lisa, A.W. Trochimczuk. *Eur. Polym. J.*, **45**, 2119 (2009).
[27] R. Jayakumar, Y.S. Lee, M. Rajkumar. *J. Appl. Polym. Sci.*, **91**, 288 (2004).

[28] M.M. Mostafa, A. El-Hammid, M. Shallaby, A.A. El-Asmy. *Transition Met. Chem.*, **67**, 303 (1981).
[29] P.F. McDermott, R.D. Walker, D.G. White. *Int. J. Toxicol.*, **22**, 135 (2003).
[30] D. Sarkar, J. Yang, A.S. Gupta, S.T. Lopina. *J. Biomed. Mater. Res. Part A*, **90A**, 263 (2009).
[31] V. Thomas, M. Jayabalan. *J. Biomed. Mater. Res. Part A*, **89A**, 192 (2009).
[32] M. Rajasekar, S. Sreedaran, R. Prabu, V. Narayanan, R. Jegadeesh, N. Raaman, A.K. Rahiman. *J. Coord. Chem.*, **63**, 136 (2010).
[33] N. Raman, A. Sakthivel, R. Jeyamurugan. *J. Coord. Chem.*, **62**, 3969 (2009).